# Glide Docking for Prediction of Potential Inhibitors of ATP7B Protein in Wilson Disease

**Monir Shalbafan[1]** iD **, Mahdieh Sadeghpour[2]✉** iD **, Abolfazl Olyaei[1]** iD

1. Department of Chemistry, Faculty of Science, Imam Khomeini International University, Qazvin, Iran
2. Department of Chemistry, Qazvin Branch, Islamic Azad University, Qazvin, Iran

## Abstract

**Background & Objectives:** Wilson's disease is a genetic disorder marked by the pathological accumulation of copper in the liver and brain due to malfunctioning of the ATP7B protein. This study employed virtual screening and glide docking techniques to explore potential therapeutic agents targeting ATP7B using natural compounds from the ZINC15 database.

**Materials & Methods:** A virtual screening protocol was implemented to rapidly identify promising drug candidates with inhibitory activity against ATP7B. The glide docking program (Schrödinger Maestro 2018-1) was used to screen natural compounds, followed by ADME analysis to assess drug-likeness and pharmacokinetic properties.

**Results:** Three lead compounds—Tobramycin, Streptomycin, and Metyrosine—were identified with the most negative G-scores and docking scores among screened compounds, signifying strong binding affinities for ATP7B. Tobramycin showed superior performance with a glide score of -6.426, accompanied by favorable ADME properties and high similarity to the reference ligand, oxaliplatin.

**Conclusion:** Tobramycin was identified as a promising candidate for therapeutic intervention in Wilson's disease, exhibiting robust binding affinity to ATP7B and drug-like characteristics. Future experimental studies are necessary to validate its clinical potential and safety.

**Keywords:** Glide docking, Wilson disease, ATP7B, Drug design, Copper transporting

## Introduction

Copper is essential for numerous physiological processes; however, excessive accumulation can lead to severe toxicity and health complications (1). Maintaining a balanced copper concentration in cells is critical for normal cellular function and the prevention of copper-related disorders. Dysregulation of copper transport, often caused by malfunctions in specific proteins,

is a key factor in several diseases, including Wilson disease (WD) (2-4). ATP7B, a copper-transporting ATPase, plays a central role in regulating copper uptake, distribution, and storage, preventing harmful accumulation in vital organs such as the liver and brain (5).

Mutations in the ATP7B gene underlie WD, leading to copper buildup that manifests as a range of symptoms, including hepatic dysfunction, neurological deficits, and psychiatric disturbances (6, 7). These debilitating effects underscore the importance of understanding ATP7B's function in copper metabolism and

✉**Corresponding Author: Sadeghpour Mahdieh,** Department of Chemistry, Qazvin Branch, Islamic Azad University, Qazvin, Iran.
**Email:** mahdieh.sadeghpour@qiau.ac.ir
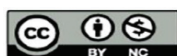
its role in disease pathology.

Ongoing research continues to explore ATP7B and related copper-transporting proteins, with the aim of developing effective therapeutic strategies for WD and similar conditions (8). One promising avenue is the multi-target ligand drug design strategy, which leverages computational tools and high-throughput screening techniques to streamline the drug discovery process. This approach facilitates the identification of safer and more effective medications for complex diseases driven by multifaceted molecular mechanisms (9-14). By integrating computational methods—such as molecular docking, binding energy calculations, and pharmacokinetic analysis—with experimental validation, researchers can identify and develop novel drug candidates targeting ATP7B. This represents a significant advancement in the quest for WD therapies (15-20).

This study investigates the potential of natural compounds as inhibitors of ATP7B, employing the computational glide docking method. By examining the active site of the ATP7B protein, this research aims to deepen our understanding of its function and its interactions with ligands. Such insights are not only crucial for the treatment of WD but also have implications for targeting copper-related pathways in cancer therapy (21-25). Potential therapeutic strategies may involve either restoring ATP7B functionality or designing drugs that modulate its activity, ultimately improving the quality of life for individuals affected by WD.

Glide docking, a computational technique widely used in virtual screening, allows researchers to predict the binding modes and affinities of small molecules with target proteins (21-25). By generating multiple ligand conformations and evaluating their interactions with the target, this method efficiently screens vast compound libraries to identify promising drug candidates. The high reliability accuracy and rapidity of glide docking make it an indispensable tool in drug discovery, enabling researchers to prioritize compounds for experimental validation and accelerating the development of novel therapeutics (21-25).

## Materials and Methods

The crystal structure of the ATP7B protein (PDB ID: 7si7) was obtained from the RCSB Protein Data Bank(https://www.rcsb.org/structure/7SI7). The structure was refined using the Protein Preparation Wizard in Schrödinger Maestro (version 11.8, 2018), (https://www.schrodinger.com/platform/products/maestro/). Refinement steps included adding hydrogen atoms, forming disulfide bonds, and removing water molecules beyond 3.00 Å from heteroatoms. Missing loops and side chains were reconstructed using the Prime module, and heteroatom states were generated using Epik. Protonation states were assigned at pH 7.00 using Propka, with further adjustments made using the software's default settings. The structure was then optimized and minimized with the OPLS3 force field.

Over 110,000 natural product ligands were retrieved from the ZINC15 database (http://www.zinc.docking.org/browse/catalogs/naturalproducts). These structures were processed with the LigPrep tool in Maestro, where the OPLS3 force field was applied to convert two dimensional (2D) structures into three dimensional (3D) forms and minimize computational errors. Ionization states were determined using Epik at pH 7.00, generating up to four isomers per ligand.

To define the active binding site of ATP7B, receptor grid generation in Maestro was employed, focusing on residues Asp1024, Asp1273, Thr1292, and Gly1274. The SiteMap module validated the generated grid box at coordinates (X: -10.06, Y: 12.95, Z: 68.49) with a midpoint box size of 10 Å. Site maps with scores exceeding 1.00 were considered valid.

Ligand docking was performed in two stages using the Glide module. First, High Throughput

Virtual Screening (HTVS) rapidly evaluated a large number of ligands. Next, the top 10% of poses underwent precise docking using the XP method. Flexible ligand sampling was applied during both steps, with docking scores used as the primary evaluation metric.

The free binding energy of ligand-protein complexes was calculated using the Molecular Mechanics Generalized Born Surface Area (MM-GBSA) and Molecular Mechanics Poisson-Boltzmann Surface Area (MM-PBSA) methods. These calculations were performed using the Prime MM-GBSA module in Maestro with the OPLS3e force field, employing the formula:

$$\Delta G_{binding} = G_{complex} - (G_{ligand} + G_{receptor})$$

Pharmacokinetics, ADME properties (Absorption, Distribution, Metabolism, and Excretion), and drug-likeness were evaluated using the QikProp application (http://www.swissadme.ch/). Final hit compounds were selected based on Lipinski's Rule of Five (RO5), polar surface area (PSA), and oral absorption percentage.

## Results

This study aimed to identify potential inhibitors of ATP7B (PDB ID: 7si7) using molecular modeling. Docking studies were conducted in Schrödinger Maestro (version 11.8, 2018) with Glide's XP mode to validate the molecular docking results. The primary objective was to identify ligands with the most favorable docking scores, indicative of strong binding affinity to ATP7B. Docking scores, which reflect computational predictions of ligand binding strength, must undergo experimental validation for confirmation.

The virtual screening process was conducted in five stages. Initially, High Throughput Virtual Screening (HTVS) identified 1,120 compounds with docking scores ranging from -7.636 to -3.837 kcal/mol. Subsequently, the XP docking mode refined this pool to more accurately predict ligand affinities. The Induced Fit Docking (IFD) protocol was then applied to account for both ligand and receptor flexibility, resulting in a shortlist of 49 compounds. These were further evaluated based on ADME properties, Lipinski's Rule of Five, and bioavailability, yielding three lead compounds. Pharmacokinetic properties of these compounds are summarized in Table 1, and their interactions with ATP7B are illustrated in Figures 1–4.

Three hit compounds—Tobramycin, Streptomycin, and Metyrosine—emerged as promising ATP7B inhibitors. Tobramycin exhibited the highest G-score of -6.426 kcal/mol, forming eight hydrogen bonds (Figure 1).

**Table 1.** ADMET properties of best docking ligands against ATP7B (PDB ID: 7si7)

| Entry | Ligand | Molecular weight (g/mol) | Num. rotatable bonds | Log Po/w | Num. H-bond acceptors | Num. H-bond donors | Log S | Pharmacoki-netics | Drug likeness Lipinski |
|-------|--------|--------------------------|----------------------|----------|----------------------|-------------------|-------|-------------------|------------------------|
| 1 | Tobramycin | 467.51 | 6 | 1.46 | 14 | 10 | 1.58 | P-gp substrate | No; 2 violations |
| 2 | Carboplatin | 371.25 | 2 | 0.00 | 6 | 4 | 1.55 | GI absorption: High | Yes; 0 violation |
| 3 | Streptomycin | 581.57 | 11 | -1.15 | 15 | 14 | 1.80 | P-gp substrate | No; 3 violations |
| 4 | Metyrosine | 195.22 | 3 | 0.97 | 4 | 3 | 0.02 | GI absorption: High | Yes; 0 violation |
| 5 | Oxaliplatin | 397.29 | 1 | 0.00 | 6 | 4 | 0.99 | GI absorption: High | Yes; 0 violation |
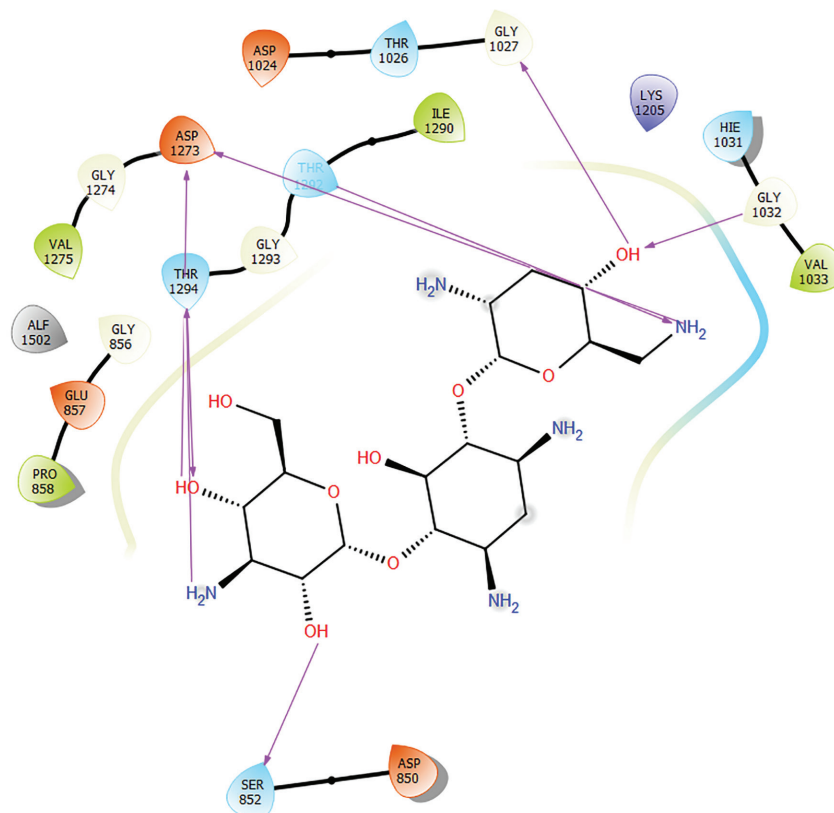
**Figure 1.** 2D stick diagram of Tobramycin illustrating hydrogen bonds formed with the amino acid residues at the binding pocket of ATP7B
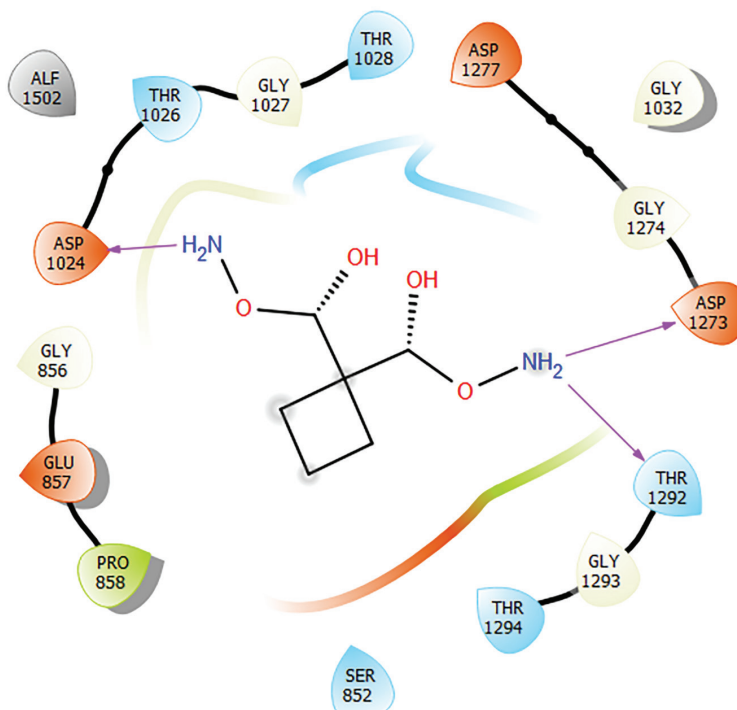


**Figure 2.** 2D stick diagram of Carboplatin illustrating hydrogen bonds formed with the amino acid residues at the binding pocket of ATP7B
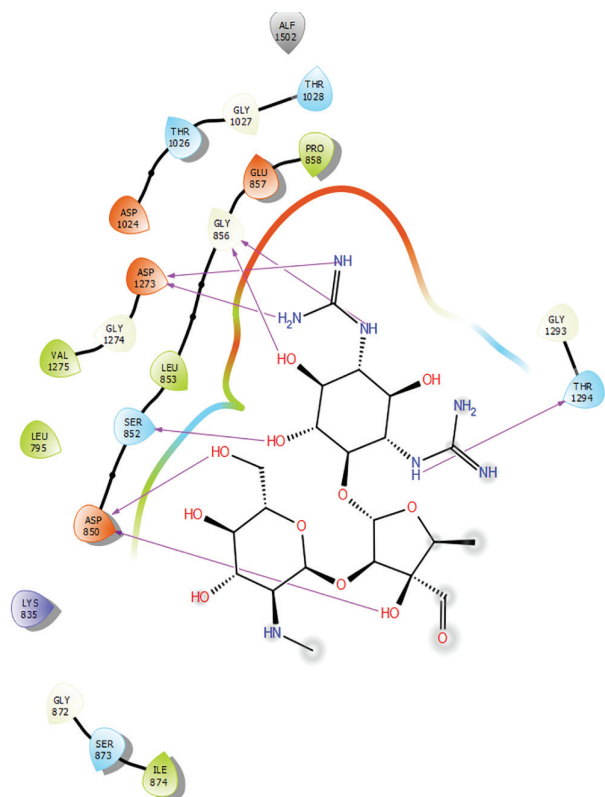
**Figure 3.** 2D stick diagram of Streptomycin illustrating hydrogen bonds formed with the amino acid residues at the binding pocket of ATP7B
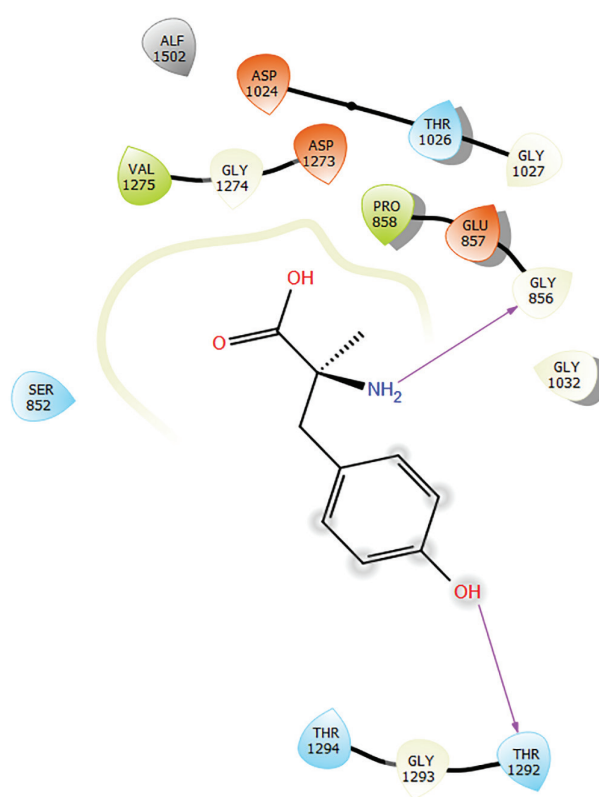


**Figure 4.** 2D stick diagram of Metyrosine illustrating hydrogen bonds formed with the amino acid residues at the binding pocket of ATP7B

In comparison, the standard ligand Carboplatin displayed a G-score of -6.377 kcal/mol with three hydrogen bonds (Figure 2). Streptomycin and Metyrosine showed binding affinities with G-scores of -6.267 and -6.23 kcal/mol, respectively (Figures 3 and 4).

Key interactions, including hydrogen bonding, hydrophobic interactions, van der Waals forces, and electrostatic interactions, contributed to the stability and high binding affinity of these drug-protein complexes. These interactions, detailed in Table 2, highlight the therapeutic potential of the identified compounds. For instance, most ligands, including approved drugs, formed hydrogen bonds with Asp1273—a critical residue in ATP7B's active site.

The mechanism of action likely involves robust binding to ATP7B, facilitated by a combination of intermolecular forces that stabilize the ligand-protein complex. This stability enhances the therapeutic efficacy of the compounds, making them promising candidates for further development in the treatment of Wilson disease.

## Discussion

The selection of the 3 compounds was based on their superior docking scores, which indicate a higher likelihood of effective binding to the ATP7B protein. Tobramycin, in particular, showed promising results in the ADME analysis, highlighting its potential as a therapeutic agent for Wilson's Disease. From these virtual screening experiments here performed, we selected the 50-ranked hits from zinc15-database. Additionally, the ADME screening helps filter out compounds that may have unfavorable pharmacokinetic properties, narrowing down the selection of promising candidates.

Table 2. Schrodinger maestro docking score (kcal/mol) of compounds against ATP7B (PDB ID: 7si7)

| Entry | zinc_ID of compound | Drug name | G score | Dock score | Lipophilic score | H-bond score |
|-------|---------------------|-----------|---------|------------|------------------|--------------|
| 1 | ZINC000008214692 | Tobramycin | -6.426 | -6.426 | -0.221 | -1.13 |
| 2 | carboplatin | carboplatin | -6.377 | -6.377 | 0 | -0.594 |
| 3 | ZINC000008214681 | streptomycin | -6.267 | -6.267 | -0.102 | -0.942 |
| 4 | ZINC000000000693 | Metyrosine | -6.23 | -6.23 | -0.134 | -0.778 |
| 5 | ZINC000000000693 | Metyrosine | -6.096 | -6.096 | -0.078 | -0.773 |
| 6 | ZINC000008214681 | streptomycin | -6.094 | -6.094 | -0.105 | -1.021 |
| 7 | ZINC000008214681 | streptomycin | -6.048 | -6.048 | -0.081 | -0.972 |
| 8 | ZINC000000000693 | Metyrosine | -5.987 | -5.987 | -0.056 | -0.77 |
| 9 | ZINC000003830405 | cefazolin | -5.861 | -5.861 | -0.295 | -0.549 |
| 10 | ZINC000001035331 | Ribavirin | -5.722 | -5.722 | 0 | -0.396 |
| 11 | ZINC000001529323 | Methotrexate | -5.657 | -5.657 | 0 | -0.31 |
| 12 | ZINC000001035331 | Ribavirin | -5.628 | -5.628 | 0 | -0.32 |
| 13 | ZINC000016929327 | Decitabine | -5.559 | -5.559 | 0 | -0.368 |
| 14 | ZINC000003977952 | Lactulose | -5.484 | -5.484 | -0.051 | 0 |
| 15 | ZINC000008214692 | Nebramycin | -5.457 | -5.457 | -0.217 | -0.885 |
| 16 | ZINC000003833821 | Prednisolone | -5.381 | -5.381 | -0.282 | -0.423 |
| 17 | ZINC000003977952 | Lactulose | -5.369 | -5.369 | -0.083 | 0 |
| 18 | ZINC000003875560 | Methylprednisolon | -5.356 | -5.356 | -0.257 | -0.423 |
| 19 | oxaliplatin | oxaliplatin | -5.347 | -5.347 | 0 | -0.699 |
| 20 | ZINC000003977952 | Lactulose | -5.333 | -5.333 | -0.027 | 0 |
| 21 | ZINC000001035331 | Ribavirin | -5.243 | -5.243 | 0 | -0.281 |
| 22 | ZINC000004658290 | Mercaptopurine | -5.211 | -5.211 | 0 | -0.18 |
| 23 | ZINC000001529323 | Methotrexate | -5.192 | -5.192 | -0.008 | 0 |
| 24 | ZINC000001530775 | entamidine | -5.174 | -5.174 | -0.345 | -0.561 |
| 25 | ZINC000003830405 | Cefazolin | -5.147 | -5.147 | -0.386 | -0.537 |
| 26 | ZINC000001530775 | Pentamidine | -5.14 | -5.14 | -0.515 | -0.5 |
| 27 | ZINC000003875560 | Methylprednisolone | -5.12 | -5.12 | -0.211 | -0.146 |
| 28 | ZINC000002005305 | Levomefolic acid | -5.099 | -5.099 | -0.489 | -0.288 |
| 29 | ZINC000004658290 | mercaptopurine | -5.097 | -5.097 | 0 | -0.15 |
| 30 | ZINC000000896546 | flucytosine | -5.058 | -5.058 | 0 | -0.227 |
| 31 | ZINC000000006226 | Deferiprone | -4.977 | -4.977 | 0 | 0 |
| 32 | ZINC000003833821 | prednisolone | -4.968 | -4.968 | -0.134 | -0.144 |
| 33 | ZINC000003830405 | Cefazolin | -4.958 | -4.958 | -0.446 | -0.06 |
| 34 | ZINC000038212689 | Fluorouracil | -4.939 | -4.939 | 0 | -0.16 |
| 35 | ZINC000016929327 | Decitabine | -4.93 | -4.93 | 0 | -0.578 |
| 36 | ZINC000100071256 | Tranexamic acid | -4.924 | -4.924 | 0 | -0.304 |
| 37 | ZINC000000001758 | mycophenolic acid | -4.883 | -4.883 | -0.352 | -0.1 |
| 38 | ZINC000003875560 | Methylprednisolone | -4.86 | -4.86 | -0.146 | -0.143 |
| 39 | ZINC000004658290 | mercaptopurine | -4.857 | -4.857 | 0 | 0 |
| 40 | ZINC000001529323 | Methotrexate | -4.846 | -4.846 | -0.131 | -0.325 |
| 41 | ZINC000003830264 | aztreonam | -4.837 | -4.837 | -0.005 | -0.146 |
| 42 | ZINC000000001758 | mycophenolic acid | -4.823 | -4.823 | -0.34 | -0.053 |
| 43 | ZINC000096006020 | paclitaxel | -4.807 | -4.807 | -0.751 | -0.122 |
| 44 | ZINC000038212689 | Fluorouracil | -4.743 | -4.743 | 0 | -0.106 |
| 45 | ZINC000000897244 | Sulbactam | -4.741 | -4.741 | 0 | 0 |
| 46 | ZINC000003918087 | doxorubicin | -4.737 | -4.737 | -0.105 | -0.329 |
| 47 | ZINC000000896546 | flucytosine | -4.724 | -4.724 | 0 | -0.146 |
| 48 | ZINC000004468780 | cefotaxime | -4.713 | -4.713 | -0.228 | -0.77 |
| 49 | ZINC000000057147 | Zinc sulfate | -4.709 | -4.709 | -0.062 | -0.176 |

Their ADME properties were compared to those of drugs currently being tested with Wilson disease. Our assay comprised of natural compounds to understand their ability as ATP7B inhibitor through in silico study. Tobramycin had a greater G score (-6.426) than the standard drug (carboplatin) used against ATP7B protein but based on the pharmacokinetic information and Lipinski's laws, the most similar is based on the absorption mechanism related to Metyrosine drug. While experimental validation would be necessary to confirm Metyrosine 's efficacy as an ATP7B inhibitor for Wilson disease, its metal ion binding properties, structural similarities to known inhibitors, established safety profile, virtual screening and molecular docking studies and potential for repurposing make it a promising candidate for further investigation through clinical studies.

## Conclusion

This study evaluated the therapeutic potential of natural compounds for Wilson's disease by utilizing molecular docking and ADME analysis. The ADME screening assessed key pharmacokinetic properties such as bioavailability, distribution, metabolic stability, and excretion, facilitating the identification of promising drug candidates. Among the screened compounds, three hits—Tobramycin, Streptomycin, and Metyrosine—exhibited the most negative G-scores and docking scores, signifying strong binding affinities to ATP7B. These compounds emerged as potential inhibitors of ATP7B, with Tobramycin showing the strongest binding affinity.

Tobramycin, Streptomycin, and Metyrosine demonstrated superior binding affinities and lower free energy values compared to the standard ligand, oxaliplatin, achieving glide scores of -6.426, -6.267, and -6.23, respectively. Notably, Tobramycin outperformed Carboplatin (standard drug) in docking metrics, forming a greater number of hydrogen bonds and displaying

a more negative docking score. A comparative analysis of these three hit compounds with a co-crystallized ligand and a standard inhibitor highlighted their strong binding interactions with ATP7B (Table 1).

The drug-likeness of the hit compounds was evaluated using Lipinski's Rule of Five. All three compounds exhibited drug-like characteristics, including molecular weights under 500 Da, fewer than five hydrogen bond donors, fewer than ten hydrogen bond acceptors, and octanol-water partition coefficients below five. Their pharmacokinetic parameters were within acceptable ranges. Tobramycin, in particular, demonstrated the highest similarity to Carboplatin in terms of P-glycoprotein (P-gp) substrate properties, making it a standout candidate for further development.

A detailed analysis of ligand-protein interactions revealed that hydrogen bonding, hydrophobic interactions, van der Waals forces, and electrostatic interactions collectively contributed to the stability and strong binding affinity of the drug-protein complexes. These findings underscore the therapeutic potential of these compounds in targeting ATP7B for the treatment of Wilson's disease.

However, these results are based on computational predictions and require experimental validation. Future studies should prioritize in vitro and in vivo experiments to confirm the strength and efficacy of these interactions and to establish the clinical potential of Tobramycin, Streptomycin, and Metyrosine for treating Wilson's disease.

## Acknowledgements

## Conflicts of interest

The authors declare no conflicts of interest.

**Authors' Contribution**

All authors contributed to the conception and design of the study. Material preparation, data collection, and analysis were performed by Monir Shalbafan. The first draft of the manuscript was written by Mahdieh Sadeghpour, and all authors provided feedback on previous versions of the manuscript. All authors reviewed and approved the final manuscript.

**References**

1 Letelier M E, Lepe A M, Faundez M, Salazar J, Marin R, Aracena P, et al. Possible mechanisms underlying copper-induced damage in biological membranes leading to cellular toxicity. Chem Biol Interact. 2005; 151(2): 71–82.

2 Dzebo M M, Arioz C, Wittung-Stafshede P. Extended functional repertoire for human copper chaperones. Biomol Concepts. 2016; 7(1): 29–39.

3 Prashanth L, Kattapagari K K, Chitturi R T, Baddam V R R, Prasad L K. A review on role of essential trace elements in health and disease. J Dr NTR Univ Health Sci. 2015; 4(2): 75–85.

4 Pham A N, Xing G W, Miller C J, Waite T D, Fenton-like copper redox chemistry revisited: Hydrogen peroxide and superoxide mediation of copper-catalyzed oxidant production. J Catal. 2013; 301: 54–64.

5 Banci L, Bertini I, Ciofi-Baffoni S, Kozyreva T, Zovo K, Palumaa P. Affinity gradients drive copper to cellular destinations. Nature. 2010; 465: 645–648.

6 Lutsenko S, Barnes N L, Bartee M Y, Dmitriev O Y. Function and regulation of human copper-transporting ATPases. Physiol Rev. 2007; 87: 1011–1046.

7 Huster D, Lutsenko S. The distinct roles of the N-terminal copper-binding sites in regulation of catalytic activity of the Wilson's disease protein. J Biol Chem. 2003; 278(34): 32212–32218.

8 Tudor Lucian P, Alina G. New developments in the management of Wilson's disease in children. J Global Pediatrics. 2024; 8: 100142-100145.

9 Abdolmaleki A, Ghasemi J B, Ghasem F. Computer aided drug design for multi-target drug design: SAR /QSAR, molecular docking and pharmacophore methods. Curr Drug Targets. 2017; 18: 556–575.

10 Alcaro S, Bolognesi M L, García-Sosa A T, Rapposelli S. Multi-target-directed ligands (MTDL) as challenging research tools in drug discovery: from design to pharmacological evaluation. Front Chem. 2019; 7:1-2.

11 Bottegoni G, Veronesi M, Bisignano P, Kacker P, Favia A D, Cavalli A. Development and Application of a Virtual Screening Protocol for the Identification of Multitarget Fragments. Chem Med Chem. 2016; 11: 1259–1263.

12 Cummings J L. Dementia and geriatric cognitive disorders: 30 yyears of publishing high-Quality research findings on cognitive dysfunction studies. Geriatr Cognit Disord. 2020; 49: 22–37.

13 Jang ES, Choi HY, Ki M, Kim BH, Kim KA, Jeong SH. A case of autoimmune hepatitis after occupational exposure to N,N-dimethyl formamide. J Korean Med Sci. 2024; 12: 1-39.

14 Scarpino A, Ferenczy G G, Keserű G M. Comparative evaluation of covalent docking tools. Curr Pharm Biotechnol. 2020; 26(44): 5684-5699.

15 Sivula T, Yetukuri L, Kalliokoski T, Käsnänen Heikki A, Pöhner P I. Machine learning-boosted docking enables the efficient structure-based virtual screening of giga-scale enumerated chemical libraries. J Chem Inf Model. 2023; 63 (18): 5773-5783.

16 Sai M, Vietor J, Kornmayer M, Egner M, López-García Ú, Höfner G, et al. Structure-guided design of nurr1 agonists derived from the natural ligand dihydroxyindole. J Med Chem. 2023; 66(19): 13556-13567.

17 Jiang D, Zhao H, Du H, Deng Y, Wu Z, Wang J, et al. How good are current docking programs at nucleic acid-ligand docking? A comprehensive evaluation. J Chem Theory Comput. 2023; 19 (16): 5633-5647.

18 Hawash M, Jaradat N, Sabobeh R, Abualhasan M, Qaoud M T. New thiazole carboxamide derivatives as COX inhibitors: design, synthesis, anticancer screening, in silico molecular docking, and ADME profile studies. ACS Omega. 2023; 8 (32): 29512-29526.

19 Zala M, Vora J J, Khedkar V M. Synthesis, Characterization, antitubercular activity, and molecular docking studies of pyrazolylpyrazoline-clubbed triazole and tetrazole hybrids. ACS Omega. 2023; 8 (23): 20262-20271.

20 Hsu D J, Davidson R B, Sedova A, Glaser J. A high-hrotughput binding pose refinement workflow through induced-fit ligand docking. J Chem Inf Model. 2023; 63 (11): 3438-3447.

21 Friesner R A, Banks J L, Murphy R B, Halgren T A, Klicic J J, Mainz D T, et al. Glide: a new approach for rapid, accurate docking and scoring.

1. Method and assessment of docking accuracy. J Med Chem. 2004; 47: 1739–1749 .

22 Sandor M, Kiss R, Keseru G M. Virtual fragment docking by Glide: a validation study on 190 protein-fragment complexes. J Chem Inf Model. 2010; 50: 1165–1172.

23 Bathula R, Muddagoni N, Lanka G, Dasari M, Potlapally S R. Glide docking, autodock, binding free energy and drug-likeness studies for prediction of potential inhibitors of cyclin-dependent kinase 14

protein in wnt signaling pathway. Biointerface Res Appl Chem. 2022; 12 (2): 2473 – 2488.

24 Mateev E, Georgieva M, Zlatkov A. Pyrrole as an Important Scaffold of Anticancer Drugs: Recent Advances. Biointerface Res Appl Chem. 2023; 13 (2): 159-169.

25 Ban T, Ohue M, Akiyama Y. Multiple grid arrangement improves ligand docking with unknown binding sites: Application to the inverse docking problem. Comput Biol Chem. 2018; 73, 139-146.